Circularly Symmetric Companding Quantization-Inspired Hybrid Constellation Shaping for APSK Modulation to Increase Power Efficiency in Gaussian-Noise-Limited Channel

ALEKSANDRA Ž. JOVANOVI [1], (Member, IEEE), IVAN B. DJORDJEVIC[2], (Fellow, IEEE),
ZORAN H. PERI [1], AND SLOBODAN A. VLAJKOV[1]

[1]Faculty of Electronic Engineering, University of Niš, 18000 Niš, Serbia
[2]Department of Electrical and Computer Engineering, The University of Arizona, Tucson, AZ 85721, USA

Corresponding author: Aleksandra Ž. Jovanović (aleksandra.jovanovic@elfak.ni.ac.rs)

ABSTRACT In this paper we address hybrid probabilistic-geometric constellation shaping (HCS) of amplitude phase shift keying (APSK) constellation based on the reversed model of optimal companding quantization for circularly symmetric sources with the goal to increase the constellation power efficiency in Gaussian-noise-limited channel. To empirically optimize the proposed APSK constellation such that a symbol-error rate (SER) reaches its minimum under given constraints with respect to signal-to-noise ratio (SNR) and the prior probabilities of constellation points, for various settings of constellation parameters, we investigate SER dependence on SNR and determine the constellation parameters achieving minimum SER. The SER dependence on SNR we estimate theoretically by deriving approximate formula for SER of uncoded APSK constellation in Gaussian-noise-limited channel and practically by performing simulation. The obtained results are well-matched verifying the accuracy of approximate SER formula. The results also show that our APSK constellation outperforms some previous APSK and M-ary QAM constellations in terms of power efficiency. Thus, for SER equal to 10^{-6} the gain in power efficiency amounts up to 2.35 dB, 2.23dB and 1.64 dB compared with the maximum mutual information-optimized $4+12$-APSK, $4+12+16$-APSK and $4+12+20+28$-APSK constellations, respectively. This means that by employing APSK constellation we propose instead the traditional APSK constellations the transmitted signal power can be reduced by a third enabling lower power consumption. The improved power efficiency of our APSK constellation makes it suitable for application in power-limited communications such as fiber-optic communications, satellite communications, power-line communications, and multiple-input multiple-output wireless transmissions.

INDEX TERMS AWGN channels, constellation diagram, digital modulation, signal detection, vector quantization.

I. INTRODUCTION

Amplitude phase shift keying (APSK) is a higher-order constellation consisting of several concentric rings, with each ring containing constellation points (modulated signals assigned to symbols) that are separated by a constant phase offset. APSK is an attractive modulation format due to its spectral and power efficiency combined with robustness against nonlinear distortion [1]–[12]. Thus, the usage of APSK is suitable to enhance performance of transmission

over nonlinear channels. For these reasons APSK has been included in the second generation of standard for digital video broadcasting via satellite, DVB-S2 [3]. Also, APSK modulation can be appropriate modulation format in fiber-optic communication systems to deal with the fiber nonlinearities [9]–[12]. Further, in a certain number of papers, differential and non-coherent spatial modulations relying on the APSK were developed for multiple-input multiple-output (MIMO) systems [13]–[17].

As communication systems increasingly demand better spectral and power efficiency of transmission techniques, the constellation shaping has drawn more attention

The associate editor coordinating the review of this manuscript and approving it for publication was Chengpeng Hao .

[1]–[15], [18]–[22]. Under constellation shaping the methods that optimize modulation format by adjusting the geometric-space location and *a priori* probabilities of constellation points are assumed. All these methods are categorized within three constellation shaping schemes: geometric constellation shaping (GCS), probabilistic constellation shaping (PCS) and hybrid probabilistic-geometric constellation shaping (HCS) [20], [21].

GCS employs a uniform distribution (equiprobable constellation points) on non-equidistant constellation points. GCS of APSK can be achieved by increasing in a non-linear way the radius of constellation ring starting from the constellation center. It is common that more constellation points are located near the constellation center than at its periphery to approximate Gaussian distribution and generate two-dimensional Gaussian-like constellation. Such geometric-space location of constellation points are usually obtained by optimizing some metrics, like minimum Euclidean distance, mutual information (MI), generalized MI [1], [2], [6], [21].

PCS imposes a non-uniform distribution (non-equiprobable constellation points) on a set of equidistant constellation points. Actually, PCS shapes the prior probabilities of constellation points rather than their locations to approximate Gaussian signaling. Specifically, PCS reduces the average transmitted power and error rate by sending low-amplitude constellation points with a higher probability than the high-amplitude ones. Thereby, due to circular symmetry of APSK constellation the constellation points under the same amplitude ring are sent equally likely [20], [21]. The non-equal probabilities are commonly generated according to the Maxwell-Boltzmann (MB) distribution, which is a Gaussian distribution sampled at discrete amplitudes across a finite amplitude range [22]. MB distribution maximizes the entropy under an average-power constraint, not the achievable information rate (AIR), so that the AIR is usually further improved by using the Blahut-Arimoto algorithm [23], [24].

Recently, PCS has started to be realized through the constellation compression by reducing the number of constellation points [18], [19]. The basic principle of novel PCS is to transfer the constellation points from the outer ring to the ones of the inner ring changing the constellation order, structure and constellation point probabilities. After constellation compression, the order of constellation is decreased, whereby the constellation points are non-uniformly distributed having higher probabilities for the constellation points of the inner rings.

Finally, when more flexible constellation format is required, HCS can be an enabling method since it does not limit constellation points to equal probabilities or equidistant location. Actually, in HCS the shaping is performed both geometrically and probabilistically resulting in non-uniform distribution (non-equiprobable constellation points) on non-equidistant constellation points. Combinations of PCS

and GCS have been considered to be implemented in optical communications to combat fiber nonlinearities [25], [26].

In this paper, we focus our research on HCS of APSK constellation with the goal to increase the constellation power efficiency in Gaussian-noise-limited channels. Instead of optimizing channel metrics or minimum Euclidean distance, which is commonly utilized methodology, we apply quantization designing methods in APSK constellation shaping. Namely, there is similarity between APSK constellation and circularly-symmetric quantization in the sense that both divide the two-dimensional geometric space into concentric rings having points separated by constant phase. This similarity motivates us to utilize advantages of quantization designing methods in HCS. Vector quantization inspired constellation designs were also proposed in several papers to perform HCS [27]–[31]. In those papers, the geometric space presentation of various models of vector quantization was directly mapped into constellation diagram. That results that the constellations from [27]–[31] are characterized with higher density of constellation points having higher prior probabilities which represents the main drawback of those constellations. From the quantization point of view, it is a desirable feature since it leads to smaller mean-squared error. However, from the standpoint of modulation and error performances, the desirable feature regarding the density of constellation points and their prior probabilities is opposite. Because of that, we conclude that in our research we should focus to achieve the space partition reversed with that in two-dimensional quantization, specifically, reversed with the circularly-symmetric quantization. To provide the above mentioned we introduce a novel concept that employs the quantization designing methods in constellation shaping on a totally different manner.

The quantization studying for a many years enabled us to notice that the quantization model for which it is easily to determine the reversed geometric-space partition is companding quantization that consists of compressor characterized by compression function, uniform quantizer and expander specified by expanding function that is inversed with the compression function. Namely, in companding quantization the output levels and thus the space partition are determined by applying the expanding function on uniformly spaced levels. This means that the reversed geometric-space partition on radius levels can be obtained by applying compression function on uniformly spaced levels. This observation motivates us to formulate the geometric shaping function as compression function of companding quantization and to specify the probabilistic shaping function as expression that determines the probabilities of radius levels in the reversed model with companding quantization, i.e. in the model consists of expander, uniform quantizer and compressor. Specifically, since we consider HCS of APSK constellation being a circularly-symmetric constellation, we opt to use the radial compression function of optimal companding quantization for circularly symmetric sources [32] to specify geometric

shaping function. Similar principle was only utilized in [33], where design of one-dimensional constellation - pulse amplitude modulation (PAM) based on optimal scalar companding quantization was proposed.

To achieve highly-structured constellation and to reduce detection complexity, apart the aforementioned features, we assume that each ring of our APSK constellation carries the same number of points. This property can be beneficial for labelling based on the multilevel coding [8].

The HCS of APSK based on novel concept we propose leads to constellations having different features in respect not only to vector quantization-inspired constellations from [27]–[31], but in respect to any other APSK constellation. The constellation we obtain has lower density of radius levels with higher prior probabilities, whereby, unlike to usual principle in constellation shaping, more constellation rings are located at constellation periphery than near its center. These features provide that our APSK constellation outperforms in terms the power efficiency the standard solutions for mutual information maximization-optimized APSK constellation having equiprobable constellation points and different numbers of constellation points associated per rings [1]–[3], [5]. To confirm the advantages arisen by using the novel concept in HCS, in numerical results we are going to extend the comparative analysis on the product-APSK constellation whose rings are packed away from the center, recently proposed in [8].

In order to estimate the power efficiency of the proposed APSK constellation, we evaluate the constellation error performances by deriving an asymptotic formula for symbol-error rate (SER) of uncoded APSK constellation in additive white Gaussian noise (AWGN) channel. Thereby, we consider receiver based on maximum a posteriori probability (MAP) criterion that leads to the complicate decision boundaries for the decision regions, known as Voronoi cells in equiprobable case. Moreover, due to the complicated decision boundaries, error performance analysis of APSK signals is more difficult than that of QAM signals. The issue of SER determining for M-ary constellation in AWGN channel was solved in [34], [35], where an union bound on SER was derived by decomposing SER calculation on calculation of M-1 pair-wise probabilities of erroneous detection for every constellation point. However, the calculation of all $M \times (M$-1$)$ pair-wise probabilities becomes cumbersome for high-order constellations. In [36]–[38] the simplified SER expressions were derived for APSK constellations from [1]–[3], [5]. In this paper we simplify SER calculation for the case when APSK constellation has different *a priori* constellation points probabilities associated per rings, but equal number of points on each ring. For the assumed scenario we simplify the union bound on SER by exploiting the symmetry properties of APSK constellation and by including only the pair-wise probabilities of erroneous detection for the neighborhood constellation points to the transmitted constellation points since the pair-wise probability decreases with constellation point distance increasing. To verify the accuracy of the

derived SNR formula we perform simulation in program package MATLAB and obtain that the theoretical and simulation results are well-matched. Finally, to empirically optimize our APSK constellation we determine SER for various settings of constellation parameters and select the constellation parameters leading to the minimum SER under considered constraints related to signal-to-noise ratio (SNR) value and *a priori* constellation point probabilities.

II. APSK CONSTELLATION SHAPING INSPIRED BY COMPANDING QUANTIZATION FOR CIRCULARLY-SYMMETRIC SOURCES

In this section we define a novel method for APSK constellation design that includes both the geometric and probabilistic shaping and results in an M-ary APSK constellation with L non-equidistant concentric rings each having N constellation points whose *a priori* probabilities are constant within the ring. We start research by defining APSK constellation as set of M pairs composed of complex representation of constellation point $(r_i \exp\{j\theta_{i,k}\})$ and its *a priori* probability (P_i)

$$C = \left\{ \left(r_i \exp\left\{ j\theta_{i,k} \right\}, P_i \right) : 1 \leq i \leq L, 1 \leq k \leq N \right\}, \quad (1)$$

where $L \times N = M$ and

$$N \sum_{i=1}^{L} P_i = 1. \quad (2)$$

In APSK constellation, due to circular symmetry, the phase offset between the adjacent constellation points that belong the same ring is constant and amounts $2\pi/N$. Thereby, also due to symmetry, the best phase offset between the adjacent rings with respect to minimum Euclidean distance maximization amounts π/N [1]. In accordance with this, we define the phase of constellation point $\theta_{i,k}$, $i = 1, \ldots, L$, $k = 1, \ldots, N$ as follows

$$\begin{aligned} \theta_{i,k} &= \vartheta\,(i, k, N) \\ &= \begin{cases} \dfrac{2\pi}{N}\left(k - \dfrac{1}{2}\right), & i = 1, 3, 5, \ldots, k = 1, \ldots, N \\ \dfrac{2\pi}{N}\,(k - 1), & i = 2, 4, 6, \ldots, k = 1, \ldots, N \end{cases} \end{aligned}$$
$$(3)$$

To specify radii of constellation points we introduce geometric shaping function that from a set of uniformly spaced radii $\{(i - 1/2)d, i = 1, 2, .., L\}$ generates a set of nonuniformly spaced ones $\{r_i, i = 1, 2, .., L\}$. Let's recall now that we conclude the issue of constellation designing is reversed with the issue of quantization designing. For that reason, we utilize companding quantization technique on inverse manner in constellation design. Namely, in companding quantization the output levels are determined by applying expanding function on uniformly spaced levels. In such manner it is achieved that the density of output levels decreases with decreasing the probability of levels. Opposite to that, in this paper, we propose that the radii of constellation

points are obtained by applying compression function on uniformly spaced levels. This provides that the density of radius levels increases with the decrease of *a priori* constellation point probability. Therefore, we define the geometric shaping function as a compression function of companding quantization. Since we consider circularly-symmetric APSK constellation the radial compression function of optimal companding quantization for circularly symmetric sources from [32] is imposed as a good choice for constellation shaping function formulation. Actually, by modifying radial compression function proposed in [32] so that it maps $[0, r_{\max}]$ into $[0, r_{\max}]$ instead to maps $[0, +\infty)$ into $[0, 1)$ and after that by performing the map of equidistant levels $(i - 1/2) \times d$, where $d = r_{\max}/L$, we derive a novel geometric shaping function for radius level determining

$$
\begin{aligned}
r_i &= \phi\left(i, L, r_{\max}\right) \\
&= r_{\max} \frac{\sqrt{1 - \exp\left\{-\frac{(i-1/2)^2 r_{\max}^2}{4L^2}\right\}}}{\sqrt{1 - \exp\left\{-\frac{r_{\max}^2}{4}\right\}}}, \quad i = 1, \dots, L. \quad (4)
\end{aligned}
$$

As we have already denoted in formula for geometric shaping function (4), GCS we propose depends only on the number of radius levels L and on the parameter $r_{\max}$.

To specify the probability that constellation point from a given radius level is transmitted $P_i^l = N \times P_i$, we introduce a function that from a set of equiprobable probability mass functions (PMFs) $\{1/L, i = 1, 2, .., L\}$ generates a set of non-equiprobable PMFs $\{P_i^l = N \times P_i, i = 1, 2, .., L\}$. The P_i^l actually denotes the PMF for the *i*th radius level r_i. To formulate the probabilistic shaping function we also utilize the analogy with model reversed with companding quantization. The model reversed with optimal companding quantization for circularly symmetric sources assumes that the two-dimensional random variable composed from two independent Gaussian random variables is fed to the cascade consisted from expander, uniform quantizer and compressor. In particular, we assume that the sum of the prior probabilities of constellation points belonging to the radius level specified by radius r_i ($P_i^l = N \times P_i$) represents the probability that radius of two-dimensional random variable composed from two independent Gaussian variables is within $[t_i, t_{i+1})$, where t_i is determined by using here proposed geometric shaping function as follows

$$
\begin{aligned}
t_i &= \phi\left(i - 1/2, L, r_{\max}\right), \quad i = 1, \dots, L \\
t_{L+1} &= +\infty
\end{aligned} \quad (5)
$$

The mathematical formulation of previous assumption can be written as

$$
P_i^l = N P_i = \exp\left\{-\frac{t_i^2}{2}\right\} - \exp\left\{-\frac{t_{i+1}^2}{2}\right\}, \quad i = 1, \dots, L. \quad (6)
$$

By substituting (5) in (6) and after that by calculating P_i we derive a novel probabilistic shaping function

$$
\begin{aligned}
P_i &= \omega\left(i, N, L, r_{\max}\right) \\
&= \begin{cases}
\frac{1}{N}\left(\exp\left\{-\frac{\phi^2\left(i - 1/2, L, r_{\max}\right)}{2}\right\}\right. \\
\left.\quad - \exp\left\{-\frac{\phi^2\left(i + 1/2, L, r_{\max}\right)}{2}\right\}\right), \\
\quad i = 1, \dots, L - 1 \\
\frac{1}{N}\exp\left\{-\frac{\phi^2\left(L - 1/2, L, r_{\max}\right)}{2}\right\}, \\
\quad i = L
\end{cases}
\end{aligned} \quad (7)
$$

Eqs. from (4) to (7) point out that in the constellation model that we propose the number of constellation points associated per ring N influences the prior probabilities of constellation points P_i, $i = 1, 2, \dots, L$, but does not the PMFs of radius levels P_i^l, $i = 1, 2, \dots, L$. From (7) one can also conclude that PCS is conditioned on GCS defined by (4). Expressions (4) and (7) point out that APSK constellation we develop has the following feature: the lower density of radius levels, the higher *a priori* probabilities of constellation points (see Fig. 1). Actually, Fig. 1(a) shows that in our constellation, unlike to common space distribution of radius levels, more constellation radius levels are located at the constellation periphery rather than near its center. Also, Fig. 1(b) indicates that, opposite to the current state in HCS, the constellation radius level on the largest distance from the adjacent levels has the highest *a priori* probability. These features are expected to enable reduction of the symbol-error rate and improvement of power-efficiency.

Finally, we can state our circularly-symmetric APSK constellation is code book defined as

$$
\begin{aligned}
C = \Big\{ &\left(r_i \exp\left\{j\theta_{i,k}\right\}, P_i\right) \Big| \\
&r_i = \phi\left(i, L, r_{\max}\right), \theta_{i,k} = \vartheta\left(i, k, N\right), P_i = \omega\left(i, N, L, r_{\max}\right): \\
&1 \le i \le L, 1 \le k \le N \Big\},
\end{aligned} \quad (8)
$$

where $\phi(i, L, r_{\max})$, $\vartheta(i, k, N)$ and $\omega(i, N, L, r_{\max})$ are defined with (4), (3) and (7), respectively. The average energy per bit of our APSK constellation estimated by applying the basic definition for the average energy per bit [34] is:

$$
\begin{aligned}
E_b &= \frac{N \sum_{i=1}^{L} P_i r_i^2}{\log_2 M} \\
&= \frac{N}{\log_2 N + \log_2 L} \sum_{i=1}^{L} \omega\left(i, N, L, r_{\max}\right) \phi^2\left(i, L, r_{\max}\right).
\end{aligned} \quad (9)
$$

One can highlight that L, N and $r_{\max}$ are the constellation parameters that can be chosen depending on target performance. This means that constellation design we propose has high degree of freedom. With L and $r_{\max}$ we influence the radius level within which N constellation points are further
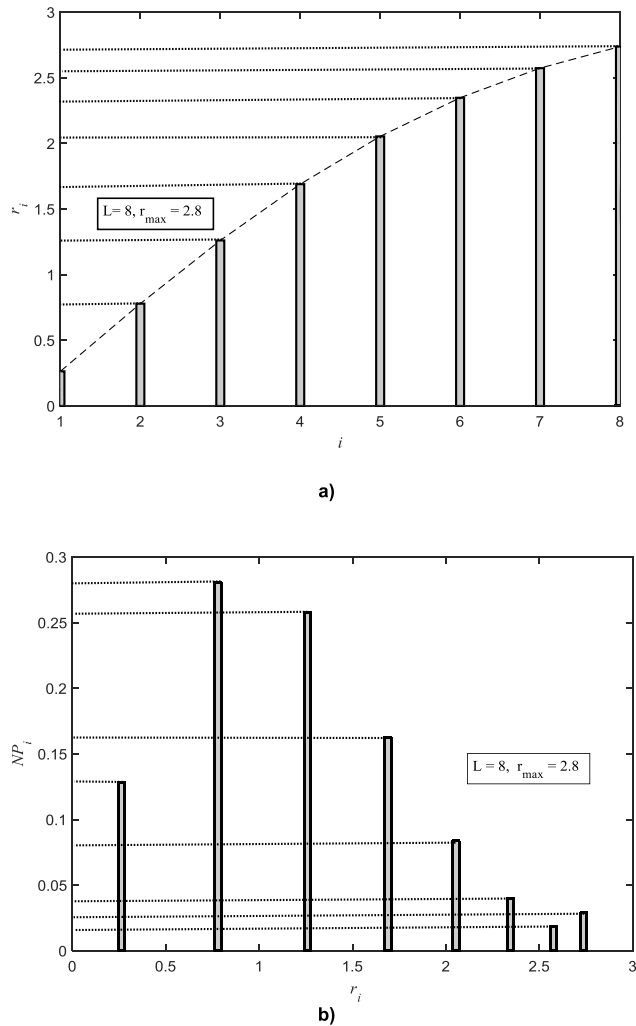
FIGURE 1. a) Constellation point radius in function of the ordinal number of the ring level; b) Constellation point probability dependence on constellation point radius.

uniformly distributed. With L and r_{max} we also control radius level PMF (P_i^l), while with N we adjust the total number of constellation points M and their *a priori* probabilities (P_i). Additionally, since it holds $M = L \times N$, the number of constellation points M is not constraint on the power of 2. For different L, N and r_{max} we determine r_i and $\theta_{i,k}$ by utilizing (4) and (3) and present the obtained constellation diagrams in Fig. 2.

III. SYMBOL-ERROR RATE FOR MAP DETECTION OF NO-CODED APSK CONSTELLATION IN AWGN CHANNEL

Let C be APSK constellation defined by (8). Assume that $\mathbf{x} = r_x \exp\{j\theta_x\} \in C$ modulates symbol transmitted through an AWGN channel. The modulated signal is affected by the AWGN with power spectral density $N_0/2$. Then, the received signal is given by

$$\mathbf{y} = \mathbf{x} + \mathbf{n} \tag{10}$$

where $\mathbf{n}$ is the AWGN component distributed according to a circular complex Gaussian distribution $CN(0, N_0/2)$. The

received signal is processed by the MAP receiver. MAP receiver investigates all $P(\mathbf{x}_{i,k}|\mathbf{y})$, $i = 1, 2, \ldots, L$, $k = 1, 2, \ldots, N$ and selects $\mathbf{x}_{i,k} = a_i \exp\{j\theta_{i,k}\}$ that maximizes $P(\mathbf{x}_{i,k}|\mathbf{y})$ [34]

$$\mathbf{x}^* = \arg\max_{\mathbf{x}_{i,k}} P\left(\mathbf{x}_{i,k} \mid \mathbf{y}\right). \tag{11}$$

By using Bayes' rule, the above decision rule can be simplified as follows [32]

$$\mathbf{x}^* = \arg\max_{\mathbf{x}_{i,k}} p\left(\mathbf{y} \mid \mathbf{x}_{i,k}\right) P\left(\mathbf{x}_{i,k}\right), \tag{12}$$

where $P(\mathbf{x}_{i,k}) = P_i$ is the prior probability of constellation point, defined by (7), while the conditional probability density function (conditional pdf) $p(\mathbf{y}|x_{i,k})$ is the probabilistic description of the AWGN channel. From (10) follows that $p(\mathbf{y}|\mathbf{x}_{i,k})$ is the joint density of two independent Gaussian random variables having the same variance ($N_0/2$) and the different mean values $r_i \cos\theta_{i,k}$ and $r_i \sin\theta_{i,k}$. This implies that the decision region for each point, except for the points from the first and last radius levels, is irregular hexagon obtained by putting normal lines on lines that connect the observed constellation point $\mathbf{x}_{i,k}$ with the nearest neighbours at the distances from the observed point

$$t_{i,k,l,m} = \frac{d_{i,k,l,m}}{2} + \frac{N_0}{d_{i,k,l,m}} \ln\frac{P_i}{P_l},$$
$$\text{for } \forall l, m \therefore \mathbf{x}_{l,m} \in N\left(\mathbf{x}_{i,k}\right). \tag{13}$$

In (13) $N(\mathbf{x}_{i,k})$ denotes the set of the nearest neighbours for the constellation point $\mathbf{x}_{i,k}$, while $d_{i,k,l,m}$ is the Euclidean distance between the constellation points $\mathbf{x}_{i,k}$ and $\mathbf{x}_{l,m}$

$$d_{i,k,l,m} = \left[r_i^2 + r_l^2 - 2r_i r_l \cos\left(\theta_{i,k} - \theta_{l,m}\right)\right]^{\frac{1}{2}}. \tag{14}$$

An additional explanation on the decision region is given in Fig. 3. One can also note that (13) reduces to $d_{i,k,l,m}/2$ for $l = i$. This means that the decision boundaries between constellation points belonging to the same circle are normal lines putted at the middle between points.

To evaluate the error performance for the assumed scenario, we start with the basic definition for SER [34] applied to the circularly-symmetric constellation

$$\text{SER} = \sum_{i=1}^{L}\sum_{k=1}^{N} P\left(e \mid \mathbf{x}_{i,k}, C\right) P_i, \tag{15}$$

where $P(e|\mathbf{x}_{i,k}, C)$ denotes the probability that the wrong symbol is detected under condition that the symbol $\mathbf{x}_{i,k}$ is transmitted and that the constellation is defined by C. The conditional symbol error probability $P(e|\mathbf{x}_{i,k}, C)$ can be expresses as:

$$P\left(e \mid \mathbf{x}_{i,k}, C\right) = P\left(\bigcup_{l=1}^{L}\bigcup_{m=1}^{N}{}_{l\neq i \vee m\neq k} E\left(\mathbf{x}_{l,m} \mid \mathbf{x}_{i,k}, C\right)\right),$$
$$\tag{16}$$

where $E(\mathbf{x}_{l,m}|\mathbf{x}_{i,k}, C)$ denotes the event that the symbol $\mathbf{x}_{l,m}$ is detected under condition that the symbol $\mathbf{x}_{i,k}$ is transmitted
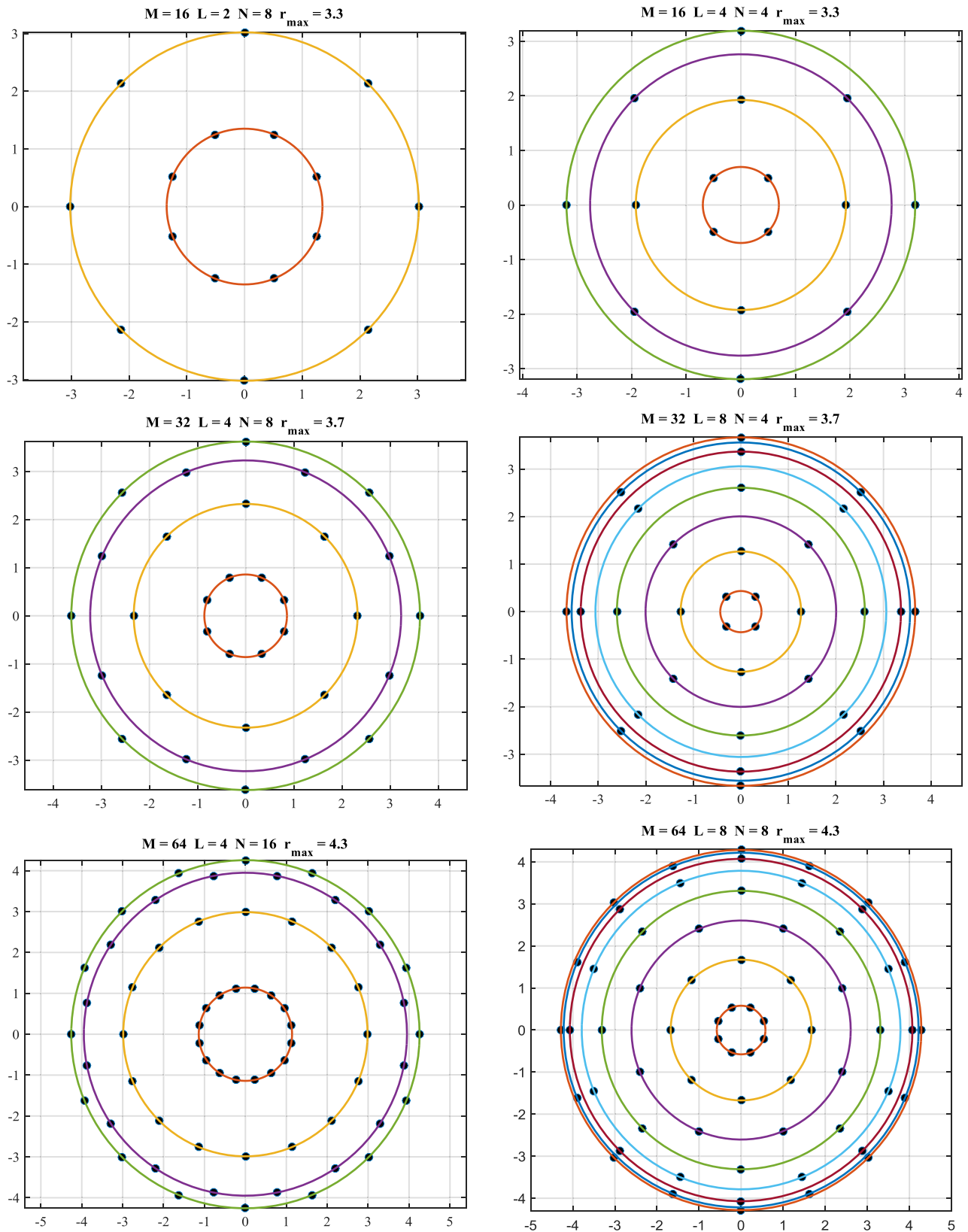
FIGURE 2. For different values of *L*, *N* and r_{max} the APSK constellation diagram.
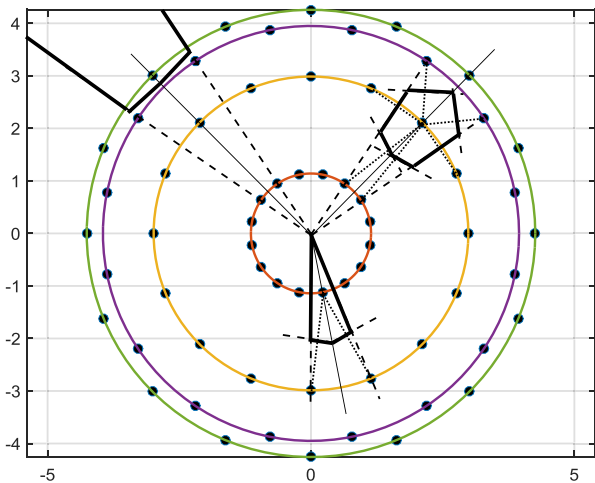
FIGURE 3. Illustration for decision regions of MAP receiver for an APSK constellation.

whereby all possible constellation points are defined by (8). One should observe the probability that $\mathbf{x}_{l,m}$ is detected if $\mathbf{x}_{i,k}$ is transmitted without taking into consideration the other constellation points (the pire-wise probability of erroneous detection) is higher than the probability if the constraint arises from C is accounted $P(E(\mathbf{x}_{l,m}|\mathbf{x}_{i,k}, C)) \leq P(E(\mathbf{x}_{l,m}|\mathbf{x}_{i,k}))$. Therefore, the upper bound on the conditional symbol error probability (16) can be specified as follows

$$P\left(e|\mathbf{x}_{i,j}, C\right) \leq \sum_{l=1}^{L} \sum_{m=1}^{N} {}_{l\neq i \vee m\neq k} P\left(E\left(\mathbf{x}_{l,m}|\mathbf{x}_{i,k}\right)\right). \quad (17)$$

By substituting (17) in (15) we obtain

$$\text{SER} \leq \sum_{i=1}^{L} \sum_{k=1}^{N} \sum_{l=1}^{L} \sum_{m=1}^{N} {}_{l\neq i \vee m\neq k} P_i P\left(E\left(\mathbf{x}_{l,m}|\mathbf{x}_{i,k}\right)\right). \quad (18)$$

By approximating SER with (18) we simplify SER calculation. Namely, SER calculation for two-dimensional constellation is decomposed on calculation of $M \times (M-1)$ error probabilities for binary signals, i.e. on calculation of $M \times (M-1)$ pire-wise probabilities of erroneous detection. It is known that in MAP detection the error probability for binary signals, here denoted with $\mathbf{x}_{i,k}$ and $\mathbf{x}_{l,m}$, in function of their Euclidean distance $d_{i,k,l,m}$ can be expressed as [34]

$$P\left(E\left(\mathbf{x}_{l,m}|\mathbf{x}_{i,k}\right)\right) = Q\left(\sqrt{\frac{d_{i,k,l,m}^2}{2N_0}} + \sqrt{\frac{2N_0}{d_{i,k,l,m}^2}} \ln \frac{P_i}{P_l}\right), \quad (19)$$

where $Q(\cdot)$ denotes Q-function

$$Q(x) = \int_x^{+\infty} \frac{1}{\sqrt{2\pi}} \exp\left(-\frac{t^2}{2}\right) dt. \quad (20)$$

By substituting (19) in (18) we formulate the union bound on SER of MAP detection for the circularly-symmetric constellation having non-equal *a priori* probabilities and equal

number of constellation points associated per rings

$$\text{SER} \leq \sum_{i=1}^{L} \sum_{k=1}^{N} \sum_{l=1}^{L} \sum_{m=1}^{N} {}_{l\neq i \vee m\neq k} P_i$$
$$\times Q\left(\sqrt{\frac{d_{i,k,l,m}^2}{2N_0}} + \sqrt{\frac{2N_0}{d_{i,k,l,m}^2}} \ln \frac{P_i}{P_l}\right). \quad (21)$$

One should observe that due to circular symmetry the expression for the union bound (21) can be further simplified. Namely, for given i and any k the conditional error probabilities $P(e|\mathbf{x}_{i,k}, C)$, $k = 1, 2, \ldots, N$ are equal. This allows us to simplify expression (21) on following manner

$$\text{SER} \leq N \sum_{i=1}^{L} \sum_{l=1}^{L} \sum_{m=1}^{N} {}_{l\neq i \vee m\neq k^*} P_i$$
$$\times Q\left(\sqrt{\frac{d_{i,k^*,l,m}^2}{2N_0}} + \sqrt{\frac{2N_0}{d_{i,k^*,l,m}^2}} \ln \frac{P_i}{P_l}\right), \quad (22)$$

where k^* denotes an arbitrary chosen value for k. In comparison to (21), the number of sum terms is reduced N times, i.e. the number of sum terms is decreased from $M \times (M-1)$ to $L \times (M-1)$. Furthermore, since the Q function is a decreasing function of its variable, the contribution of terms in (22) decreases with the increase of distance from the transmitted constellation point $\mathbf{x}_{i,k^*}$, $i = 1, 2, .., L$. This means that the expression (22) can be further simplified by neglecting the terms related with symbols that are not neighbours to the transmitted symbols $\mathbf{x}_{i,k^*}$, $i = 1, 2, .., L$. Beside this, one should take into account that for large N each $\mathbf{x}_{i,k^*}$ has 6 neighbours if $i = 2, .., L$-1 or 4 neighbours if $i = 1$ or $i = L$ (see Fig. 3). Thereby, the existing circular symmetry should be also included in expression simplification. Overall this gives the SER expression having only $3L-2$ sum terms:

SER
$$\approx 2NP_1 Q\left(\sqrt{\frac{d_{1,k^*,1,k^*+1}^2}{2N_0}}\right)$$
$$+ 2NP_1 Q\left(\sqrt{\frac{d_{1,k^*,2,k^*}^2}{2N_0}} + \sqrt{\frac{2N_0}{d_{1,k^*,2,k^*}^2}} \ln \frac{P_1}{P_2}\right)$$
$$+ 2N \sum_{i=2}^{L-1} P_i Q\left(\sqrt{\frac{d_{i,k^*,i-1,k^*}^2}{2N_0}} + \sqrt{\frac{2N_0}{d_{i,k^*,i-1,k^*}^2}} \ln \frac{P_i}{P_{i-1}}\right)$$
$$+ 2N \sum_{i=2}^{L-1} P_i Q\left(\sqrt{\frac{d_{i,k^*,i,k^*+1}^2}{2N_0}}\right)$$
$$+ 2N \sum_{i=2}^{L-1} P_i Q\left(\sqrt{\frac{d_{i,k^*,i+1,k^*}^2}{2N_0}} + \sqrt{\frac{2N_0}{d_{i,k^*,i+1,k^*}^2}} \ln \frac{P_i}{P_{i+1}}\right)$$

$$+ 2NP_L Q \left(\sqrt{\frac{d^2_{L,k^*,L-1,k^*}}{2N_0}} + \sqrt{\frac{2N_0}{d^2_{L,k^*,L-1,k^*}}} \ln \frac{P_L}{P_{L-1}} \right)$$

$$+ 2NP_L Q \left(\sqrt{\frac{d^2_{L,k^*,L,k^*+1}}{2N_0}} \right) \qquad (23)$$

IV. NUMERICAL RESULTS

In Section 2 we have proposed novel hybrid shaped product APSK constellation. In this section we primarily investigate the ability of the proposed constellation to preserve the fidelity/quality of digital messages at low power levels, i.e. we scrutinize constellation power efficiency by estimating $SNR = E_b/N_0$ required to achieve a given SER. Going towards this goal we analyze dependence of SER, calculated by means of formula derived in Section 3, on constellation parameters such as r_{max}, L and M. In Fig. 4 for different M and r_{max} we present SER versus L. These dependences are shown for SNR values 15 dB and 20 dB. From figure one can note the expected feature that SER increases with M. Another observation is that SER decreases, i.e. the power efficiency improves with r_{max} increasing. The parameter r_{max} influences GCS (see (4)) and PCS (see (6) and (7)). By increasing r_{max} we arrange the constellation points within wider circle and at the same time make that differences between *a priori* constellation point probabilities associated per rings become more pronounced. This means that with r_{max} increasing the ring radii become more distant, whereby the extremely high *a priori* constellation point probability and the extremely low the prior constellation point probability can occur. All these lead to lower SER.

The results presented in Fig. 4 show that SER dependence on L has minimum. In almost all cases SER minimum is achieved for $L = 4$. The optimal value for L depends on M, but also on SNR and r_{max}. Thus, for $M = 64$, when the target SNR is 15 dB, the optimal L is equal to 16, while for higher SNR value of 20dB, the SER minimum can be achieved at lower $L = 4$. Also, for $M = 16$, if r_{max} has smaller value, for example $r_{max} = 3$, then the optimum for L is 2, otherwise the optimal L is equal to 4. Since during r_{max} specifying one should have in mind that larger r_{max} means lower SER, an adequate choice for 16-APSK constellation can be constellation having $r_{max} = 3.3$ and $L = 4$. An additional request regards to r_{max} specification is that larger M implies larger r_{max}. Namely, SER degrades with M increasing, so it is necessary to increase r_{max} in order to improve somewhat SER. However, the increase of r_{max} can cause negligible small constellation point probability associated to the Lth ring (P_L) and thus the constellation size reduction. Because of that, the value for r_{max} cannot be increased indefinitely and the compromise should be made when the choice of r_{max} is in question.

In Table 1, we specify ring radii and constellation point probabilities associated per rings for several APSK constellations. In accordance with the aforementioned observations we increase r_{max} with M. In Table 1 we also tabulate SER
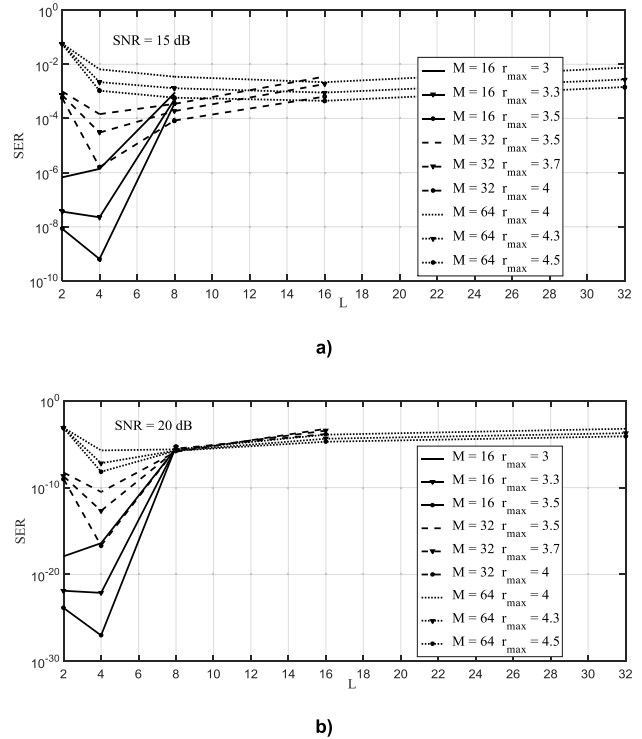

a)

b)

FIGURE 4. SER versus L for: a) SNR = 15 dB and b) SNR = 20 dB.

for different values of SNR. We determine SER by calculating approximate formula (23) and by running simulation in program package MATLAB. The obtained results indicate the well-matching between theoretical SER and simulation SER*. In such way we verify the accuracy of the derived approximate formula for SER calculation. Apart this, the results presented in Table 1 confirm observations from Fig. 4. Namely, for $M = 16$ and $r_{max} = 3.3$, APSK constellation having $L = 4$ outperforms other constellations in terms of the SER for the SNRs from Table 1. Therewith, the difference in SER is more significant when 16-APSK having $L = 4$ is compared to 16-APSK with $L = 8$ than when it is compared to 16-APSK with $L = 2$. The results presented for 32-APSK clearly indicate that the appropriate value for L is 4, while when M is 64, the optimal value for L depends on the target SNR. Thus, the optimal L is 8 for the SNRs equal to 18 dB and 19 dB, while for SNR = 20 dB the optimal L is 4, whereby the achieved SERs with both Ls are similar for all SNRs from the table.

In order to evaluate the achieved results, in Fig. 5 we present SER dependence on SNR for our APSK constellations (red curves) and some other constellations from literature. First of all, we explore SER dependence on SNR for M-ary APSK having equiprobable constellation points arranged within L equidistant concentric rings (blue curves) because these equidistant radii-equiprobable points APSK constellations are starting constellation in HCS that we perform. From Fig. 5 it is evident that HCS that we propose achieves considerable gain in terms of power efficiency compared to starting constellations since a far less SNR is necessary for

TABLE 1. Constellation parameters for several APSK constellations, SER estimated by using (23) and SER* determined by simulation.

M	r_{max}	L	N	$\mathbf{r}=\|r_1, r_2, \ldots, r_L\|$ $\mathbf{P}=\|P_1, P_2, \ldots, P_L\|$	SNR|dB|	SER	SER*
16	3.3	2	8	$\mathbf{r}=\|1.3505, 3.0225\|$ $\mathbf{P}=\|0.1180, 0.0070\|$	11 12 13	4.9309×10^{-4} 9.3739×10^{-5} 1.1879×10^{-5}	4.8780×10^{-4} 9.0900×10^{-5} 1.0700×10^{-5}
		4	4	$\mathbf{r}=\|0.6967, 1.9255, 2.7625, 3.1947\|$ $\mathbf{P}=\|0.1496, 0.0864, 0.0115, 0.0026\|$	11 12 13	3.09×10^{-4} 5.84×10^{-5} 7.39×10^{-6}	3.13×10^{-4} 6.25×10^{-5} 7.30×10^{-6}
		8	2	$\mathbf{r}=\|0.3511, 1.0315, 1.6496, 2.1757, 2.5943, 2.9047, 3.1183, 3.2544\|$ $\mathbf{P}=\|0.1078, 0.1914, 0.1226, 0.0502, 0.0171, 0.0058, 0.0022, 0.0030\|$	11 12 13	0.0050 0.0029 0.0016	0.0043 0.0025 0.0014
32	3.7	2	16	$\mathbf{r}=\|1.6508, 3.4767\|$ $\mathbf{P}=\|0.0614, 0.0011\|$	13 14 15	0.0073 0.0026 7.3451×10^{-4}	0.0073 0.0026 7.3210×10^{-4}
		4	8	$\mathbf{r}=\|0.8584, 2.3251, 3.2303, 3.6224\|$ $\mathbf{P}=\|0.0930, 0.0299, 0.0018, 2.97\times10^{-4}\|$	13 14 15	8.25×10^{-4} 1.88×10^{-4} 3.00×10^{-5}	8.26×10^{-4} 1.88×10^{-4} 2.77×10^{-5}
		8	4	$\mathbf{r}=\|0.4335, 1.2666, 2.0052, 2.6079, 3.0594, 3.3682, 3.5601, 3.6678\|$ $\mathbf{P}=\|0.0770, 0.1090, 0.0472, 0.0125, 0.0029, 0.0008, 0.0002, 0.0004\|$	13 14 15	0.0011 4.4412×10^{-4} 1.8743×10^{-4}	0.0010 4.0600×10^{-4} 1.6920×10^{-4}
64	4	2	32	$\mathbf{r}=\|1.8987, 3.8185\|$ $\mathbf{P}=\|0.0311, 0.0002\|$	18 19 20	0.0075 0.0027 7.5861×10^{-4}	0.0075 0.0027 7.7700×10^{-4}
		4	16	$\mathbf{r}=\|0.9937, 2.6480, 3.5892, 3.9416\|$ $\mathbf{P}=\|0.0522, 0.0099, 3.19\times10^{-4}, 4.26\times10^{-5}\|$	18 19 20	1.44×10^{-4} 2.08×10^{-5} 1.8824×10^{-6}	1.39×10^{-4} 2.12×10^{-5} 7.0000×10^{-7}
		8	8	$\mathbf{r}=\|0.5027, 1.4622, 2.2957, 2.9528, 3.4207, 3.7199, 3.8905, 3.9767\|$ $\mathbf{P}=\|0.0487, 0.0557, 0.0169, 0.0030, 5.25\times10^{-4}, 1.14\times10^{-4}, 3.24\times10^{-5}, 5.29\times10^{-5}\|$	18 19 20	9.2605×10^{-5} 1.6513×10^{-5} 2.4834×10^{-6}	9.0300×10^{-5} 1.6500×10^{-5} 3.4000×10^{-6}
		16	4	$\mathbf{r}=\|0.2521, 0.7504, 1.2314, 1.6850, 2.1026, 2.4777, 2.8064, 3.0872, 3.3208,$ $3.5100, 3.6589, 3.7729, 3.8575, 3.9184, 3.9609, 3.9896\|$ $\mathbf{P}=\|0.0297, 0.0677, 0.0668, 0.0446, 0.0233, 0.0104, 0.0043, 0.0017, 7.28\times10^{-4}$ $3.21\times10^{-4}, 1.51\times10^{-4}, 7.67\times10^{-5}, 4.14\times10^{-5}, 2.34\times10^{-5}, 1.37\times10^{-5}, 9.20\times10^{-5}\|$	18 19 20	2.5732×10^{-4} 1.6410×10^{-4} 1.2178×10^{-4}	2.1890×10^{-4} 1.3700×10^{-4} 1.0160×10^{-4}

the same SER. Concretely, in Table 2 we list the required SNR for SER $= 10^{-6}$. Comparing the error performances of our APSK constellations with the corresponding equidistant radii-equiprobable points APSK constellations one can note that achieved gain in power efficiency for SER equal to 10^{-6} amounts from ΔSNR $= 5.88$ dB for $M = 16$ to ΔSNR $= 11.14$ dB for $M = 64$. This means that the considerably power saving is carried out. More precisely, if the desired level of SER is 10^{-6}, the useful signal power can be reduced by $10^{5.88/10} = 3.87$ times if $M = 16$ or by $10^{11.14/10} = 13$ times if $M = 64$. By observing our and starting constellations for $L = 4$, one can note that unlike equidistant radii-equiprobable points APSK constellation in which the penalty for increasing rate $R = \log_2 M$ is 4.37 dB/bit and 5.06 dB/bit, this penalty for our APSK constellation is far less and amounts 2.62 dB and 2.71 dB/bit. The similar conclusions apply to other L values. This is one more confirmation that our APSK constellation is more power efficient compared with equidistant radii-equiprobable points APSK constellation.

From Table 2 one can note that the lowest value of SNR to achieve SER $= 10^{-6}$ is obtained for L equal to 4 if our ASPK constellation has 16 or 32 constellation points. On the other hand, the lowest SNR (for the same SER) is achieved for L equal to 8 when our APSK constellation

has 64 constellation points. These findings match the results presented in Table 1. In order to estimate the gain achieved in power efficiency with APSK constellation we propose, in Table 2 we also provide the SNR value necessary to achieve SER $= 10^{-6}$ with traditional APSK constellation. More precisely, in continuous, we compare novel APSK with standard solutions for APSK constellations having equiprobable constellation points ($P_i = const$) and different numbers of constellation points associated per rings ($N_i, i = 1, 2, \ldots, L$). Due to different numbers of points per rings the commonly adopted nomenclature for those constellations is $N_1 + N_2 + \ldots + N_L$- APSK. For those constellations, based on the mutual information maximization, the optimal relative radius and phase shift of each ring with respect to the inner ring were determined in [1]–[3], [5]. Interestingly, it was shown in [1]–[3], [5] there is no noticeable dependence on the relative phase shifts between the rings at high SNR. Therefore, only the optimal relative radii $\rho_i = r_{i+1}/r_1$, $i = 1, 2, \ldots$, L-1 were specified as function of spectral efficiency. In Table 2, for M equal to 16, 32 and 64 we list the APSK constellation parameters ($L, N_1, \ldots, N_L$) and ($\rho_1, \ldots, \rho_{L-1}$) proposed in [1]–[3], [5]. In Fig. 5 and Table 2 we also present SERs for those APSK constellations (green curves) estimated by using simplified formulas derived in [36]–[38]. The presented data show that our APSK constellations are superior
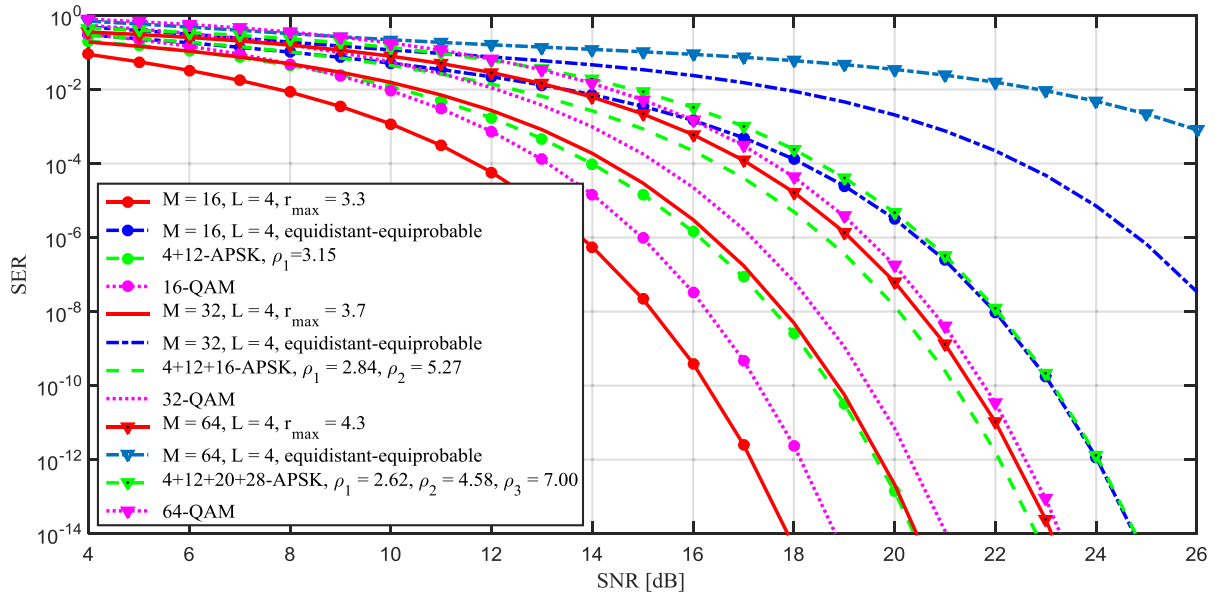
FIGURE 5. SER in function of SNR for several no-coded APSK constellations in AWGN channel.

TABLE 2. SNR required to achieve SER equal to 10^{-6}.

SER = 10^{-6}	Our APSK		Starting APSK		$N_1+N_2+\ldots+N_L$ − APSK standard			APSK[8]		QAM
M	$(L,N,r_{\max})$	SNR	(L,N)	SNR	$(L,N_1,\ldots,N_L)$	$(\rho_1,\ldots,\rho_{L-1})$	SNR	(L,N,r_0)	SNR	SNR
16	(2,8,3.3)	13.96	(2,8)	19.84		(3.15)	16.14	(2,8,1.2)	17.43	
	(4,4,3.3)	13.79	(4,4)	20.47	(2,4,12)	(2.85)	15.55	(4,4,1.5)	18.65	14.99
	(8,2,3.3)	16.30	(8,2)	23.26		(2.57)	15.38	(8,2,1.6)	24.50	
32	(2,16,3.7)	18.22	(2,16)	24.72		(2.84,5.27)	18.64	(2,16,1.2)	20.25	
	(4,8,3.7)	16.41	(4,8)	24.84	(3,4,12,16)	(2.72, 4.87)	18.26	(4,8,1.4)	19.95	17.17
	(8,4,3.7)	16.70	(8,4)	25.30		(2.53, 4.3)	17.83	(8,4,1.6)	23.53	
64	(4,16,4.3)	19.12	(4,16)	29.90		(2.62,4.58,7.00)	20.61	(4,16,1.3)	22.04	
	(8,8,4.3)	18.97	(8,8)	29.84	(4,4,12,20,28)	(2.58,4.40,6.56)	20.34	(8,8,1.5)	24.68	19.46
	(16,4,4.3)	19.10	(16,4)	30.24		(2.50,4.14,6.00)	20.12	(16,4,1.6)	29.64	

over APSK constellations proposed in [1]–[3], [5] in terms of SER and power efficiency. Concretely, for SER = 10^{-6} the gain in power efficiency achieved with our APSK ΔSNR = $\text{SNR}^{N1+N2+\ldots+NL-\text{APSK}} - \text{SNR}^{\text{our APSK}}$ goes up to 2.35 dB for $M = 16$, 2.23 dB for $M = 32$ and 1.64 dB for $M = 64$. This means that transmitted signal power can be reduced by a third, enabling lower power consumption.

Moreover, given that the novel concept and method for HCS of APSK constellation improve power efficiency of APSK constellation, the proposed constellation can be applicable in power-limited communications, such as optical communications [9]–[12], [39], [40], satellite communications [1]–[3], power-line communications and multiple-input multiple-output wireless transmissions [13]–[17].

In channels dominated by the white Gaussian noise, our APSK constellation is more power efficient than the recently proposed product-APSK constellation in [8]. Each ring of APSK constellation from [8] carries the same number of points whereby points on different rings are aligned on

semi-lines starting from the center. The adjacent rings are equidistant, but the first ring is from center on radial distance r_0. For APSK constellation from [8] we record in Table 2 the SNR required for SER = 10^{-6}. Based on the underlined data presented in Table 2 for our constellation and constellation from [8], one can conclude our APSK constellation requires from 3.64 dB to 3.07 dB lower SNR to achieve SER equal to 10^{-6}.

Finally, we compare error performances of our circular APSK constellation with square QAM constellation [34]. Fig. 5 shows that for the given $r_{\max}$ and L values our APSK constellation outperforms the M-ary QAM constellation (purple curves) in terms of power efficiency. To quantify this gain we use data presented in Table 2. By calculating difference between SNRs of M-ary QAM constellations and our constellations having $L = 4$ we obtain that the achieved gain in power efficiency ΔSNR amounts 1.2 dB for $M = 16$, 0.76 dB for $M = 32$ and 0.34 dB for $M = 64$. One can conclude that gain in power efficiency decreases with M increasing pointing out that our APSK

constellation outperforms M-ary QAM more significantly for lower M.

V. CONCLUSION

In this paper, we proposed a novel method for HCS of APSK constellation inspired by methods for companding quantization designs. Novelty of method respect to previous methods based on quantization models is reflected in establishing an analogy with the reversed model of optimal companding quantization for circularly-symmetric sources and in utilization of quantization designing method on inverse manner. In particular, the geometric shaping function is defined as the modified radial compression function of circularly-symmetric optimal companding quantization, while probabilistic shaping function is determined by establishing analogy with the probabilities of output levels in model reversed with companding quantization. This approach enabled the design of APSK constellation having 1) lower density of radius levels with higher *a priori* probabilities and 2) larger number of constellation radius levels located at constellation periphery rather than near its center and thus decreasing the SER and the significant improving the power efficiency. Compared with maximum mutual information-optimized APSK constellations, after adjusting APSK constellation parameters to minimize SER of uncoded APSK signal in Gaussian-noise-limited channel, we achieved the gain in power efficiency up to 2.35 dB for $M = 16$, 2.23 dB for $M = 32$ and 1.64 dB for $M = 64$ if SER is constrained to 10^{-6}. Our APSK constellation also outperforms M-ary QAM constellation in terms of power efficiency, whereby the power efficiency gain is more significant at lower M. Due to its improved power efficiency, the APSK constellation we proposed is suitable for use in various power-limited communications.

REFERENCES

[1] R. De Gaudenzi, A. Guillen i Fabregas, and A. Martinez, "Performance analysis of turbo-coded APSK modulations over nonlinear satellite channels," *IEEE Trans. Wireless Commun.*, vol. 5, no. 9, pp. 2396–2407, Sep. 2006.

[2] R. De Gaudenzi, A. Guillén i Fàbregas, and A. Martinez, "Turbo-coded APSK modulations design for satellite broadband communications," *Int. J. Satell. Commun. Netw.*, vol. 24, no. 4, pp. 261–281, Jul. 2006, doi: 10.1002/sat.841.

[3] European Telecommunications Standards Institute, *Digital Video Broadcasting (DVB) Second Generation: Framing Structure, Channel Coding and Modulation Systems for Broadcasting, Interactive Services, News Gathering and Other Broadband Satellite Applications*, document ETSI EN 302 307 Version 1.2.1, Aug. 2009.

[4] *Flexible Serially Concatenated Convolutional Turbo Codes With Near-Shannon Bound Performance for Telemetry Applications*, document CCSDS 131.2-O-1, CCSDS Orange Book, Sep. 2007, no. 1.

[5] K. P. Liolis and N. S. Alagha, "On 64-APSK constellation design optimization," in *Proc. 10th Int. Workshop Signal Process. Space Commun.*, Rhodes, Greece, Oct. 2008, pp. 1–7, doi: 10.1109/SPSC.2008.4686709.

[6] M. C. Valenti and X. Xiang, "Constellation shaping for bit-interleaved LDPC coded APSK," *IEEE Trans. Commun.*, vol. 60, no. 10, pp. 2960–2970, Oct. 2012, doi: 10.1109/TCOMM.2012.070912.110533.

[7] H. Meric, "Approaching the Gaussian channel capacity with APSK constellations," *IEEE Commun. Lett.*, vol. 19, no. 7, pp. 1125–1128, Jul. 2015, doi: 10.1109/LCOMM.2015.2431674.

[8] P. Ferrand, M. Maso, and V. Bioglio, "High-rate regular APSK constellations," *IEEE Trans. Commun.*, vol. 67, no. 3, pp. 2015–2023, Mar. 2019, doi: 10.1109/TCOMM.2018.2886258.

[9] B.-J. Kwak, N.-O. Song, B. Park, and D. S. Kwon, "Spiral QAM: A novel modulation scheme robust in the presence of phase noise," in *Proc. IEEE 68th Veh. Technol. Conf.*, Calgary, BC, Canada, Sep. 2008, pp. 1–5, doi: 10.1109/VETECF.2008.221.

[10] C. Hager, A. G. I. Amat, A. Alvarado, and E. Agrell, "Constellation optimization for coherent optical channels distorted by nonlinear phase noise," in *Proc. IEEE Global Commun. Conf. (GLOBECOM)*, Anaheim, CA, USA, Dec. 2012, pp. 2870–2875, doi: 10.1109/GLOCOM.2012.6503552.

[11] C. Hager, A. Graell i Amat, A. Alvarado, and E. Agrell, "Design of APSK constellations for coherent optical channels with nonlinear phase noise," *IEEE Trans. Commun.*, vol. 61, no. 8, pp. 3362–3373, Aug. 2013, doi: 10.1109/TCOMM.2013.061913.120713.

[12] Y. Han, S. Yu, M. Li, J. Yang, and W. Gu, "An SVM-based detection for coherent optical APSK systems with nonlinear phase noise," *IEEE Photon. J.*, vol. 6, no. 5, Oct. 2014, Art. no. 7100510, doi: 10.1109/JPHOT.2014.2357424.

[13] X. Jin, Q. Wu, Q. Li, W. Zhai, and N. Jin, "Design of power allocation for APSK non-coherent spatial modulation system," *Mobile Netw. Appl.*, vol. 25, no. 5, pp. 1715–1721, Oct. 2020, doi: 10.1007/s11036-020-01581-9.

[14] J. Liu, L. Dan, P. Yang, L. Xiao, F. Yu, and Y. Xiao, "High-rate APSK-aided differential spatial modulation: Design method and performance analysis," *IEEE Commun. Lett.*, vol. 21, no. 1, pp. 168–171, Jan. 2017, doi: 10.1109/LCOMM.2016.2610962.

[15] Y. Zhou, H. Zhang, P. Zhang, and D. Yuan, "Non-coherent spatial modulation and optimal multi-ring APSK constellation design," *IEEE Commun. Lett.*, vol. 22, no. 5, pp. 950–953, May 2018, doi: 10.1109/LCOMM.2018.2810876.

[16] E. Basar, M. Wen, R. Mesleh, M. Di Renzo, Y. Xiao, and H. Haas, "Index modulation techniques for next-generation wireless networks," *IEEE Access*, vol. 5, pp. 16693–16746, 2017, doi: 10.1109/ACCESS.2017.2737528.

[17] S. Sugiura, T. Ishihara, and M. Nakao, "State-of-the-art design of index modulation in the space, time, and frequency domains: Benefits and fundamental limitations," *IEEE Access*, vol. 5, pp. 21774–21790, 2017, doi: 10.1109/ACCESS.2017.2763978.

[18] L. Jiang, B. Liu, Y. Mao, X. Wu, J. Ren, X. Xu, S. Han, J. Zhao, L. Zhao, T. Sun, and L. Zhang, "A novel multi-level constellation compression modulation for GFDM-PON," *IEEE Photon. J.*, vol. 11, no. 2, pp. 1–11, Apr. 2019, doi: 10.1109/JPHOT.2019.2897315.

[19] X. Wu, B. Liu, L. Zhang, Y. Mao, X. Xu, J. Ren, L. Jiang, Y. Zhang, and X. Xin, "A probabilistic shaping method based on intrinsic bit-level labeling and asymmetric polygon modulation for optical interconnects," *Opt. Commun.*, vol. 444, pp. 68–73, Aug. 2019, doi: 10.1016/j.optcom.2019.03.028.

[20] J. Cho and P. J. Winzer, "Probabilistic constellation shaping for optical fiber communications," *J. Lightw. Technol.*, vol. 37, no. 6, pp. 1590–1607, Mar. 15, 2019, doi: 10.1109/JLT.2019.2898855.

[21] Z. Qu, I. B. Djordjevic, and J. Anderson, "Two-dimensional constellation shaping in fiber-optic communications," *Appl. Sci.*, vol. 9, no. 9, p. 1889, May 2019.

[22] F. R. Kschischang and S. Pasupathy, "Optimal nonuniform signaling for Gaussian channels," *IEEE Trans. Inf. Theory*, vol. 39, no. 3, pp. 913–929, May 1993, doi: 10.1109/18.256499.

[23] S. Arimoto, "An algorithm for computing the capacity of arbitrary discrete memoryless channels," *IEEE Trans. Inf. Theory*, vol. IT-18, no. 1, pp. 14–20, Jan. 1972, doi: 10.1109/TIT.1972.1054753.

[24] R. Blahut, "Computation of channel capacity and rate-distortion functions," *IEEE Trans. Inf. Theory*, vol. IT-18, no. 4, pp. 460–473, Jul. 1972, doi: 10.1109/TIT.1972.1054855.

[25] J.-X. Cai, H. G. Batshon, M. V. Mazurczyk, O. V. Sinkin, D. Wang, M. Paskov, W. W. Patterson, C. R. Davidson, P. C. Corbett, G. M. Wolter, T. E. Hammon, M. A. Bolshtyansky, D. G. Foursa, and A. N. Pilipetskii, "70.46 Tb/s over 7,600 km and 71.65 Tb/s over 6,970 km transmission in C+L band using coded modulation with hybrid constellation shaping and nonlinearity compensation," *J. Lightw. Technol.*, vol. 36, no. 1, pp. 114–121, Jan. 1, 2018, doi: 10.1109/JLT.2017.2757281.

[26] Z. Qu, S. Zhang, and I. B. Djordjevic, "Universal hybrid probabilistic-geometric shaping based on two-dimensional distribution matchers," in *Proc. Opt. Fiber Commun. Conf.*, San Diego, CA, USA, 2018, pp. 1–3.

[27] H. G. Batshon, I. B. Djordjevic, L. Xu, and T. Wang, "Iterative polar quantization-based modulation to achieve channel capacity in ultrahigh-speed optical communication systems," *IEEE Photon. J.*, vol. 2, no. 4, pp. 593–599, Aug. 2010, doi: 10.1109/JPHOT.2010.2051219.

[28] I. B. Djordjevic, A. Z. Jovanovic, M. Cvijetic, and Z. Peric, "Multidimensional vector quantization-based signal constellation design enabling beyond 1 Pb/s serial optical transport networks," *IEEE Photon. J.*, vol. 5, no. 4, Aug. 2013, Art no. 7901312, doi: 10.1109/JPHOT.2013.2269678.

[29] I. B. Djordjevic, A. Z. Jovanovic, Z. H. Peric, and T. Wang, "Multidimensional optical transport based on optimized vector-quantization-inspired signal constellation design," *IEEE Trans. Commun.*, vol. 62, no. 9, pp. 3262–3273, Sep. 2014, doi: 10.1109/TCOMM.2014.2347298.

[30] Z. H. Peric, I. B. Djordjevic, S. M. Bogosavljevic, and M. C. Stefanovic, "Design of signal constellations for Gaussian channel by using iterative polar quantization," in *Proc. 9th Medit. Electrotech. Conf. (MELECON)*, Tel-Aviv, Israel, vol. 2, 1998, pp. 866–869, doi: 10.1109/MELCON.1998.699349.

[31] Z. H. Peric and S. M. Bogosavljevic, "A method for exact error probability determination of nonuniform signaling for Gaussian channels," *Elektronika IR Elektrotechnika*, vol. 7, no. 49, pp. 9–12, 2003.

[32] Z. H. Perić, O. D. Milanović, and A. . Jovanović, "Optimal companding vector quantization for circularly symmetric sources," *Inf. Sci.*, vol. 178, no. 22, pp. 4375–4381, Nov. 2008, doi: 10.1016/j.ins.2008.05.029.

[33] S. Vlajkov, A. Jovanović, and Z. Perić, "Approach in companding-quantisation-inspired PAM constellation design," *IET Commun.*, vol. 12, no. 18, pp. 2305–2314, Nov. 2018, doi: 10.1049/iet-com.2018.5439.

[34] G. Proakis and M. Salehi, *Digital Communication*. New York, NY, USA: McGraw-Hill, 2008.

[35] R. Ziemer and R. Peterson, *Introduction to Digital Communications*. Upper Saddle River, NJ, USA: Prentice-Hall, 2001.

[36] W. Sung, S. Kang, P. Kim, D.-I. Chang, and D.-J. Shin, "Performance analysis of APSK modulation for DVB-S2 transmission over nonlinear channels," *Int. J. Satell. Commun. Netw.*, vol. 27, no. 6, pp. 295–311, May 2009, doi: 10.1002/sat.938.

[37] O. Afelumo, A. B. Awoseyila, and B. G. Evans, "Simplified evaluation of APSK error performance," *Electron. Lett.*, vol. 48, no. 14, pp. 886–888, Jul. 2012, doi: 10.1049/el.2012.1740.

[38] D. Shi, N. Wu, H. Wang, and J. Kuang, "Simplified error performance analysis of APSK signals," *IEICE Commun. Exp.*, vol. 3, no. 5, pp. 163–167, 2014, doi: 10.1587/comex.3.163.

[39] N. Komuro and H. Habuchi, "Intensity modulation direct detection optical wireless communication with nonorthogonal code shift keying," in *Proc. IEEE 8th Global Conf. Consum. Electron. (GCCE)*, Osaka, Japan, Oct. 2019, pp. 723–726, doi: 10.1109/GCCE46687.2019.9015538.

[40] M.-Y. Liu, T.-L. Wang, and S.-M. Tseng, "Throughput performance analysis of asynchronous optical CDMA networks with channel load sensing protocol," *IEEE Photon. J.*, vol. 9, no. 3, Jun. 2017, Art. no. 7202313, doi: 10.1109/JPHOT.2017.2677945.

IVAN B. DJORDJEVIC (Fellow, IEEE) received the Ph.D. degree from the University of Niš, Yugoslavia, in 1999.

Prior to joining The University of Arizona, he held appointments at the University of Bristol and the University of the West of England, U.K., Tyco Telecommunications, USA, the National Technical University of Athens, Greece, and State Telecommunication Company, Yugoslavia. He is currently a Professor of electrical and computer engineering and optical sciences with The University of Arizona, the Director of the Optical Communications Systems Laboratory (OCSL) and the Quantum Communications (QuCom) Laboratory, and the Co-Director of the Signal Processing and Coding Laboratory. He has authored or coauthored eight books, more than 530 journal and conference publications, and 53 U.S. patents. He is a Fellow of OSA. He serves as an Area Editor/Associate Editor/Member of Editorial Board for the following journals: IEEE COMMUNICATIONS LETTERS, OSA/IEEE JOURNAL OF OPTICAL COMMUNICATIONS AND NETWORKING, *Journal of Optics* (IOP), *Physical Communication* (Elsevier), *Optical and Quantum Electronics*, and *Frequenz*.

ZORAN H. PERI was born in Niš, Serbia, in 1964. He received the B.S., M.S., and Ph.D. degrees from the Faculty of Electronic Engineering, University of Niš, in 1989, 1994, and 1999, respectively. He was the Vice-Dean of the Faculty of Electronic Engineering for 11 years. He is currently a Full Professor with the Faculty of Electronic Engineering, University of Niš. He is a member of the council of the University of Niš. He has been a supervisor of 12 Ph.D. theses and over 80 master's and bachelor's theses and an author of 310 articles. His research results were awarded by the Telenor Foundation in 2017 for the contribution in the field of telecommunications in the category of scientific articles published over the previous two years in renowned international journals. His current research interests include the information theory, source and channel coding, signal processing, and machine learning. He has been a Reviewer of IEEE TRANSACTIONS ON INFORMATION THEORY, IEEE TRANSACTIONS ON SIGNAL PROCESSING, COMPEL, and INFORMATIKA. He has been a member of the Editorial Board of the journals *Elektronika ir Elektrotechnika*, *Information*, and *Facta Universitatis* Series: Electronics and Energetics. He serves as a Lead Guest Editor for *Information*. He was the Lead Guest Editor of special issue Advanced Signal Processing and Adaptive Learning Methods in the journal *Computational Intelligence and Neuroscience* and the Editor-in-Chief in the journal *Facta Universitatis* Series: Electronics and Energetics.

ALEKSANDRA . JOVANOVI (Member, IEEE) received the Ph.D. degree in electrical engineering from the University of Niš, Serbia, in 2007.

She is currently an Associate Professor with the Department of Telecommunications, Faculty of Electronic Engineering, University of Niš. She is an author or a coauthor of over 90 international journal/conference publications. Her research interests include source coding, signal compression, signal constellation design, and signal detection. She was awarded by Telenor Foundation in 2017 for contribution in the field of telecommunications in the category of scientific papers published over the past two years in renowned international journals. She was a Reviewer for bilateral projects and reputable journals, such as IEEE TRANSACTIONS ON COMMUNICATIONS, IEEE SIGNAL PROCESSING LETTERS, *Digital Signal Processing*, IET's journals, COMPEL, *Informatica*, *Physical Communication*, and *Computational Intelligence and Neuroscience*.

SLOBODAN A. VLAJKOV was born in Pirot, Serbia, in February 1989. He graduated in electrical engineering and computer science from the Faculty of Electronic Engineering, University of Niš, in 2013. During his studies, he had the opportunity to be an exchange student at NTNU University, Norway, for a period of one semester, in 2012. During his studies, he attended and successfully completed courses in CISCO network technology (CCN1). In parallel with his Ph.D. studies, from June 2014 to January 2018, he worked as a Process Control Engineer in a newly built plant at Tigar Tires (Michelin group). Since January 2018, he has been working as the Head of the group for achieving quality at Tigar Tires.

●●●